A Numerical Study on Thermal Drying of Moist Porous Solid

F. ZERAFAT ANGIZ, N. AMANIFARD, A. K. HAGHI*
Faculty of Engineering
The University of Guilan
P. O. Box 3756, Rasht, Iran
http://www.guilan.ac.ir

Abstract: - Drying of porous media has been the subject of many studies and is still a very active research topic. In addition to its practical importance in relation with the industrial drying of many products, drying can still be considered as an unsolved problem from a scientific standpoint. In this study, some general aspects of simultaneous heat and mass transfer in a thick porous body during drying process were investigated. The natures of solutions were discussed considering the physical properties of solid. It is shown that the temperature gradients play a role in describing the moisture profiles within the material when thickness is large. The predictions of temperature and moisture content show that the leading edge dries faster compared to other sides of the solid. Drying temperature and moisture content distributions in the porous solid were not uniform due to front stagnation effect during convection drying.

Key-Words: Heat transfer, Thermal drying, Porous solids, Moisture profile, Drying behavior

Nomenclature

β	Coefficient of thermal expansion
c	Specific heat
c^*	Specific heat of porous medium
C	Density of vapor
D_{ij}	Diffusion coefficient of moisture
g	Acceleration of gravity
h	Vapor enthalpy per mass
h_{fg}	Vapor enthalpy
h_m	Mass transfer coefficient
k	Thermal conductivity
m	Mass
M	Moisture per mass of porous medium
P	Fluid pressure
ρ	Density
t	Time
T	Temperature
T_∞	Ambient temperature
u	Components of velocity in y direction
U_∞	Uniform velocity of fluid
v	Components of velocity in x direction

1. Introduction

Drying is fundamentally a problem of simultaneous heat and mass transfer under transient conditions resulting in a system of coupled non-linear partial differential equations.

In capillary porous materials, moisture migrates through the body as a result of capillary forces and gradients of moisture content, temperature and pressure. This movement contributes to other heat transfer mechanisms while eventual phase change occurring within the material act as heat sources or sinks [1]. Kallel et al. [1] have developed a one-dimensional model for simultaneous heat and moisture transfer in porous materials. Luikov [2] and later Whitaker [3] defined a coupled system of partial differential equations for heat and mass transfer in porous bodies. Also Ben Nasrallah and perre [4]; and Murugesan et al.[5] have used one-dimensional in studying heat and mass transfer during convective drying of porous media.

Ferguson and Lewis [6] studied drying problem of timber, with a two-dimensional model. Comini and Lewis [7] have used finite element method for solution of two-dimensional heat and mass transfer in porous media.

In general, the design of dryers requires the knowledge of the drying rate as a function of the moisture content at constant conditions. As it is impossible to predict drying rates with the help of heat and mass transfer theories, the drying rates must be obtained experimentally. Hence, it seems desirable to reduce the number of experiments. This is possible with the help of models that permit to extrapolate measured drying curves on different drying conditions. To main objective of this paper is to study the drying behavior of porous solid.

2. Governing equations for porous solid

The geometry of computational field is shown in Fig.1. The problem considers a sample of rectangular porous solid exposed to convective airflow. The porous solid is assumed to be saturated with water initially.

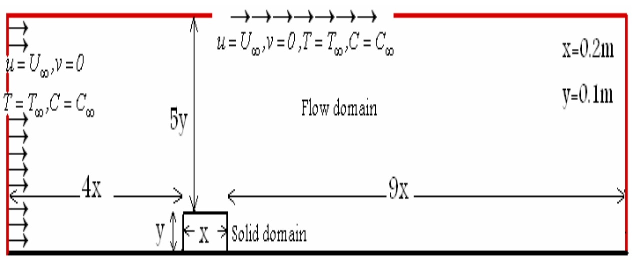

Fig.1. Geometry of computational field

The equations for porous solid phase as obtained by Kallel et al. [1] on the basis of continuum approach, were applied for numerical solution.

Energy equation :

$$c^* \frac{\partial T}{\partial t} = \left(\frac{k}{\rho_0} + h_{fg} D_{tv}\right)\left(\frac{\partial^2 T}{\partial x^2} + \frac{\partial^2 T}{\partial y^2}\right) + h_{fg} D_{mv}\left(\frac{\partial^2 M}{\partial x^2} + \frac{\partial^2 M}{\partial y^2}\right) \quad (1)$$

Where:

$$c^* = c_0 + m_l c_l + m_v c_v$$

Moisture conservation equation:

$$\frac{\partial M}{\partial t} = (D_{tl} + D_{tv})\left(\frac{\partial^2 T}{\partial x^2} + \frac{\partial^2 T}{\partial y^2}\right) + (D_{ml} + D_{mv})\left(\frac{\partial^2 M}{\partial x^2} + \frac{\partial^2 M}{\partial y^2}\right) \quad (2)$$

- Governing equations for flow field

Continuity:

$$\frac{\partial u}{\partial x} + \frac{\partial v}{\partial y} = 0 \quad (3)$$

Momentum equation (2D Navier-Stokes):

$$\frac{\partial u}{\partial t} + u\frac{\partial u}{\partial x} + v\frac{\partial u}{\partial y} = -\frac{1}{\rho}\frac{\partial P}{\partial x} + \upsilon\left(\frac{\partial^2 u}{\partial x^2} + \frac{\partial^2 u}{\partial y^2}\right) \quad (4)$$

$$\frac{\partial v}{\partial t} + u\frac{\partial v}{\partial x} + v\frac{\partial v}{\partial y} = -\frac{1}{\rho}\frac{\partial P}{\partial y} + \upsilon\left(\frac{\partial^2 v}{\partial x^2} + \frac{\partial^2 v}{\partial y^2}\right) + g\beta(T - T_\infty) + g\beta'(C - C_\infty) \quad (5)$$

Energy equation

$$\frac{\partial T}{\partial t} + u\frac{\partial T}{\partial x} + v\frac{\partial T}{\partial y} = \alpha\left(\frac{\partial^2 T}{\partial x^2} + \frac{\partial^2 T}{\partial y^2}\right) \quad (6)$$

Vapor concentration equation

$$\frac{\partial C}{\partial t} + u\frac{\partial C}{\partial x} + v\frac{\partial C}{\partial y} = D\left(\frac{\partial^2 C}{\partial x^2} + \frac{\partial^2 C}{\partial y^2}\right) \quad (7)$$

- Boundary and initial conditions

$T(x,y,0) = T_0$; $M(x,y,0) = M_0$

The boundary condition at interface of solid and fluid are:(No slip condition) $u = 0$; $v = 0$

Continuity of temperature $T_f = T_s$

Continuity of concentration $C = C(T, M)$

Heat balance:

$$(k + \rho_0 h_{fg} D_{tv})\frac{\partial T}{\partial n} + \rho_0 h_{fg} D_{mv}\frac{\partial M}{\partial n} = k_f \frac{\partial T_f}{\partial n} + h_{fg} D\frac{\partial C}{\partial n} \quad (8)$$

Species flux balance:

$$\rho_0\left(D_{tv}\frac{\partial T}{\partial n} + D_{mv}\frac{\partial M}{\partial n}\right) = D\frac{\partial C}{\partial n} \quad (9)$$

Boundary conditions for flow field are Inlet boundary condition:

$u = U_\infty$, $v = 0$, $T = T_\infty$, $C = C_\infty$

Far stream boundary condition (upper boundary):

$u = U_\infty$, $T = T_\infty$, $C = C_\infty$

Outflow boundary condition: $\frac{\partial u}{\partial x} = 0$

Also bottom surface of solid is taken adiabatic.

3. Grid dependency and solution method

A structured mesh was used for computational work. Mesh clustering around body is illustrated in Fig.2. Moisture content in leading edge obtained with three different meshes (Fig. 3).

- Solution method:

1 Solving two-dimensional flow field equations (continuity + NS) using SIMPLE algorithm and finite volume scheme.

2. Solution of energy equation for fluid using ADI technique and finite difference scheme.

3. Calculation of moisture content distribution for porous body.

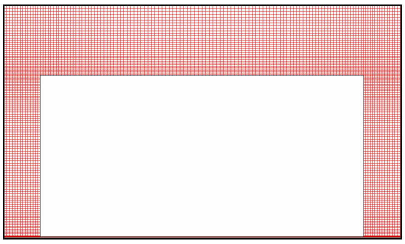

Fig.2. Mesh structure over the porous material

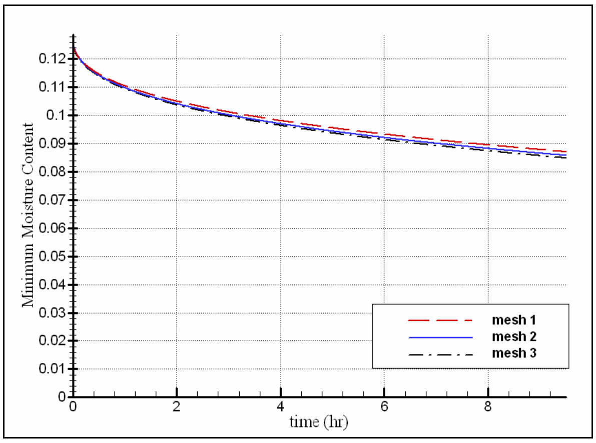

Fig.3. Moisture content in leading edge obtained with three different meshes

4. Results and discussion

In Fig. 4, drying curve of modeled solid for Re=200 is verified by results of Murugesan et al. [8].

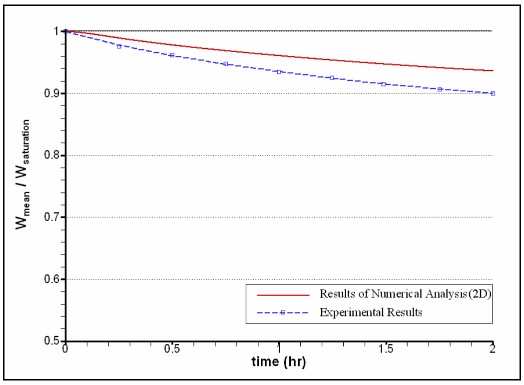

Fig.4. Drying curve of present work, and published by Murugesan et al. [8].

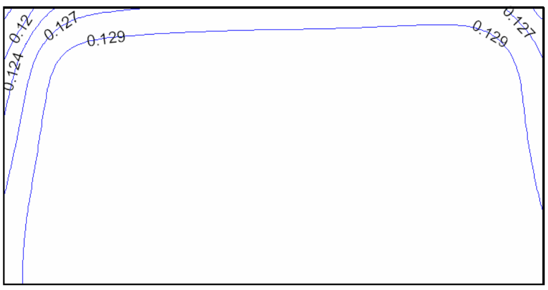

(a)

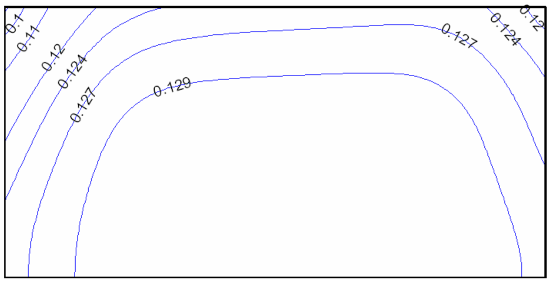

(b)

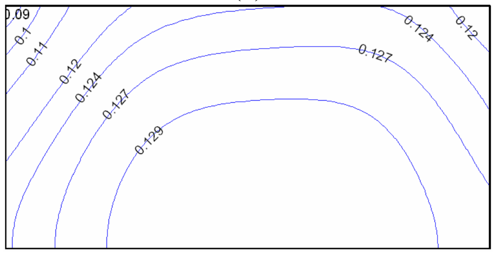

(c)

Fig 5. Moisture content distributions (kg moisture /kg dry) during drying
(a) $t = 2^1/_2$ hr (b) t = 9 hr (c) $t = 15^1/_2$ hr

The computational results of moisture content profile for Re=200 illustrates that drying rate in region near leading edge (which corresponds to maximum concentration gradient in adjacent air) is more than other regions in porous body (Figure.5).

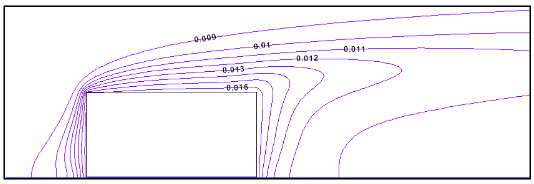

Fig.6 concentration contours in air around porous body.

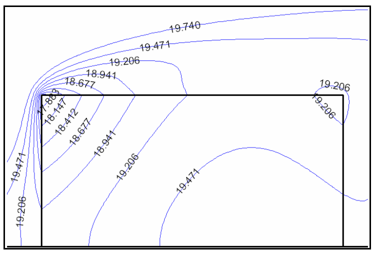

(a)

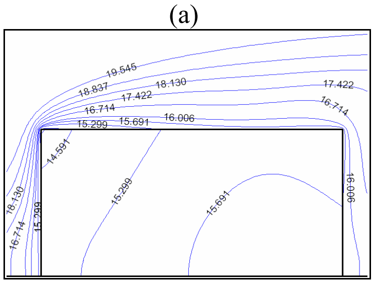

(b)

Fig.7. Temperature distributions in porous body
(a) $t = 2^1/_2$ hr (b) $t = 15^1/_2$ hr

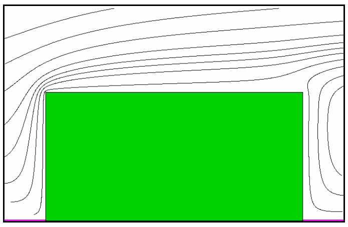

(a)

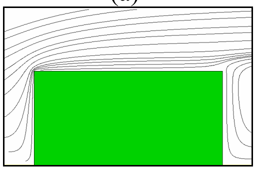

(b)

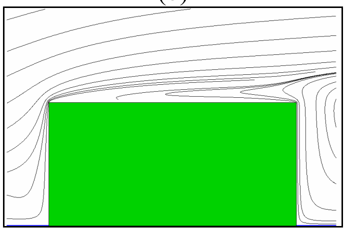

(c)

Fig.8. Streamlines for different value of Re
(a) Re_y=50 (b) Re_y=100 (c) Re_y=200

Concentration values in air around porous body are presented in Fig.6. Gradient of concentration in the body surface has shown strong effect on moisture content distribution in body (as seen for leading edge).

Temperature distributions in porous body and around air in the course of drying are shown in Fig.7. Temperature variation near leading edge decreases quickly as a result of higher moisture vaporization from surface there, and this temperature drop transfer to centric regions of porous body.

Fig.8 shows streamlines around body for Reynolds number of 50, 100 and 200.

In Fig.9, contours of concentration around body for denoted numbers of Reynolds are illustrated.

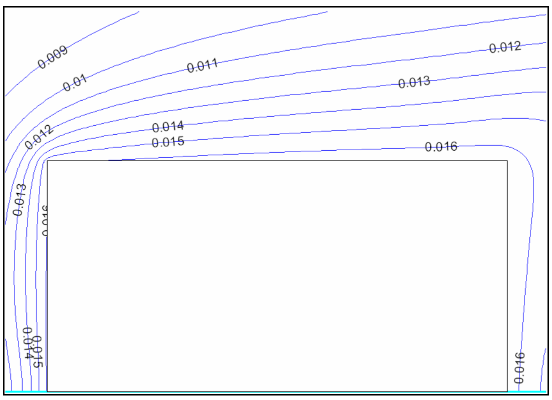

(a)

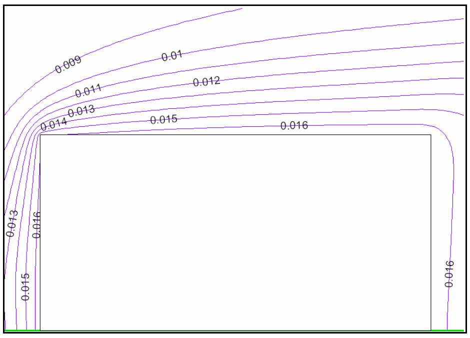

(b)

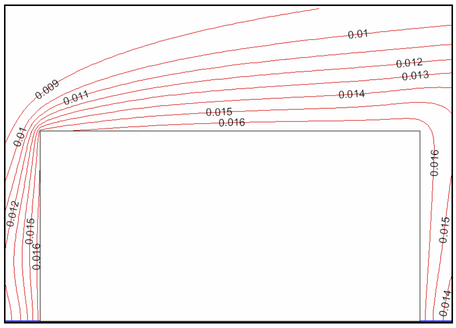

(c)

Fig.9. Concentration contours for different value of Re
(a) Re_y=50 (b) Re_y=100 (c) Re_y=200

For Re=100, moisture contents are less than those obtained for Re=50, especially for regions near by leading edge (Fig.10 (a) and (b)). This is mainly due to thinner concentration boundary layer aforementioned. In transition to Re=200 from Re=100 (Fig.10 (b) and (c)), this matter satisfies just for leading edge and left side of body (as a result of vortex formation above body in Re=200).

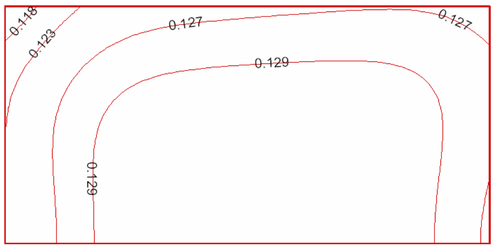

(a)

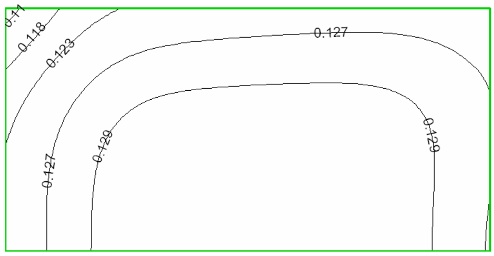

(b)

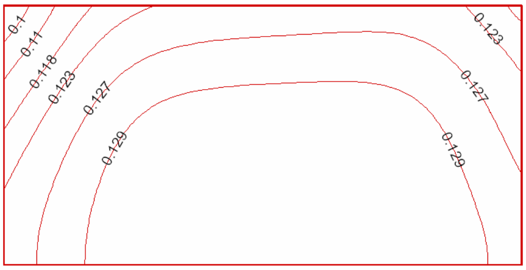

(c)

Fig.10. Moisture content contours (kg moisture /kg dry) for different value of Re
(a) Re_y=50 (b) Re_y=100 (c) Re_y=200

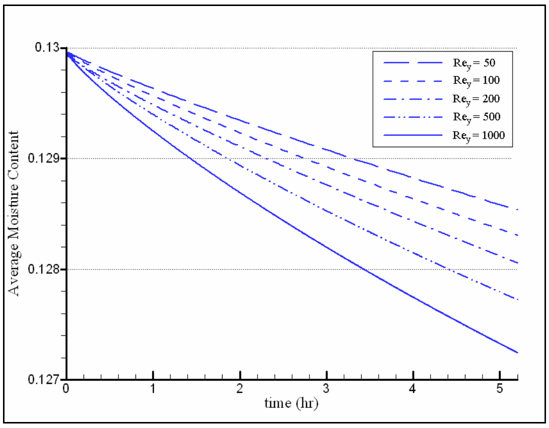

Fig.11. Drying curves for Re=50 to 1000

In Fig.11 drying curves are shown for various Reynolds number ranging from 50 to 1000. Effect of drying fluid velocity on process time could be clearly analyzed. For example, removed moisture after 5 hours of drying process for Re=100 is 15.4% more than corresponding value of Re=50. This difference is 17.5% for two Reynolds numbers of 500 and 200.

Fig.12 shows streamlines around porous body in Re=200 for both of forced and mixed convection assumptions.

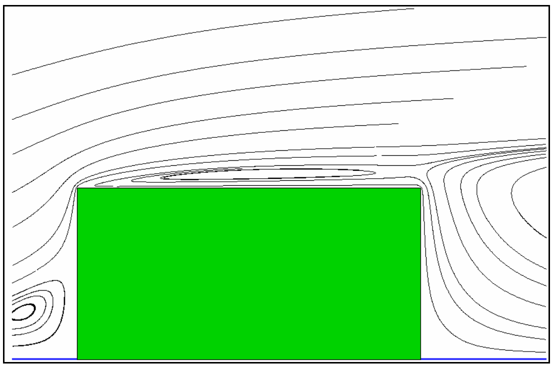

Fig.12. Effect of buoyancy forces on streamlines for Re=200

5. Conclusion

The drying behavior of moist porous solid was studied in this article. The results show that the flow due to buoyant force can be a significant external transport. This should be obviously taken into account for low Reynolds numbers. It has also been shown that the leading edge of the porous solid dries faster as compared to other regions, since the gradients of temperature and moisture are higher in that location. Meanwhile, temperature and moisture content distributions in the solid are not uniform due to front stagnation effect during convection drying.

References:

[1] Kallel, F., Galanis, N., Perrin, B., Javelas, R., 1993, Effects of moisture on temperature during drying of consolidated porous materials, J. Heat Transfer ASME Trans., Vol. 115, pp. 724-733.

[2] Luikov, A.V., 1966, Heat and mass transfer in capillary-porous bodies, Pergamon Press.

[3] Whitaker, S., 1977, Simultaneous heat, mass and momentum transfer in porous media: a theory of drying, Advances in Heat Transfer, Vol. 13, pp. 119–203.

[4] Ben Nasrallah, S., Perre, P., 1988, Detailed study of a model of heat and mass transfer during convective drying of porous media, Int. J. Heat Mass Transfer Vol. 31, No. 5, pp. 297-310.

[5] Murugesan, K., Seetharamu, K.N., Narayana, P.A.A., 1996, A one-dimensional analysis of convective drying of porous materials, Heat and Mass Transfer, Vol. 32, pp. 81-88.

[6] Ferguson, W.J., Lewis, R.W., 1991, A comparison of a fully non-linear and a partially non-linear heat and mass transfer of a timber drying problem, Proceedings of 7th Conf. on Numerical methods in Thermal Problems, Vol. VII, Part 2, pp. 973-984.

[7] Comini, G., Lewis, R.W., 1976, A numerical solution of 2D problems involving heat and mass transfer, Int. J. Heat Mass Transfer, Vol. 19, pp. 1387-1392.

[8] Murugesan, K., Suresh, H.N., Seetharamu, K.N., Narayana, P.A.A., Sundararajan, T., 2001, A theoretical model of brick drying as a conjugate problem, International Journal of Heat and Mass Transfer, Vol. 44, No. 21, pp. 4075–4086.